INSTITUTE OF PHYSICS PUBLISHING JOURNAL OF OPTICS B: QUANTUM AND SEMICLASSICAL OPTICS

J. Opt. B: Quantum Semiclass. Opt. **5** (2003) 237–242 PII: S1464-4266(03)59734-8

Single-particle quantum tunnelling in ionic traps

R M Serra, C J Villas-Bôas and M H Y Moussa

Departamento de Física, Universidade Federal de São Carlos, PO Box 676, São Carlos, 13565-905, São Paulo, Brazil

E-mail: serra@df.ufscar.br (R M Serra) and miled@df.ufscar.br (M H Y Moussa)

Received 11 February 2003
Published 22 April 2003
Online at stacks.iop.org/JOptB/5/237

Abstract
We describe a proposal to probe the quantum tunnelling mechanism of an individual ion trapped in a double-well electromagnetic potential. The time evolution of the probability of fluorescence measurement of the electronic ground state is employed to characterize the single-particle tunnelling mechanism. The proposed scheme can be used to implement quantum information devices.

Keywords: Quantum tunnelling, trapped ions, Rabi oscillations

Together with nonlocality and wavevector collapse—the phenomena behind the recent advances in quantum communication [1] and computation [2]—the tunnelling mechanism is one of the most intriguing aspects of the microscopic world of particles and their interactions, setting quantum reality apart from classical physics. While nonlocality and wavevector collapse have been pursued as clues to understanding fundamental quantum phenomena such as the uncertainty principle and the process of quantum measurement [3], quantum tunnelling is a valuable mechanism for probing the transition from quantum to classical dynamics [4].

Quantum tunnelling at the macroscopic level has attracted much attention in the literature [4–6], firstly owing to its application to SQUIDs (superconducting quantum interference devices), permitted by the advances in cryogenics, and recently because of the realization of Bose–Einstein condensation in dilute atomic gases. The observation of matter–wave interference fringes has demonstrated that a Bose condensate consists of 'laser-like' atoms which are spatially coherent and show long-range correlations, opening the field of coherent atomic beams and of atomic Josephson effect [7].

Probed at the single-particle level, quantum tunnelling is just as provocative to our intuition as its manifestation on the macroscopic scale. The experimental techniques developed over the last decade for manipulating the electronic and vibrational states of trapped ions can be employed to investigate fundamental quantum effects at a level so far accessible only as collective processes [8]. We describe in this paper a scheme for probing the tunnelling mechanism of an individual ion trapped in a double-well electromagnetic potential. The time evolution of the probability of a fluorescence measurement of the electronic ground state is used to probe the single-particle tunnelling mechanism.

(i) We first assume that the ion is trapped in a symmetric double-well single-particle potential $V(x) = b(x^2 - x_0^2)^2$. (In ionic traps, the typical oscillation frequencies in the y and z directions are very much larger than that in the x direction, providing a good approximation to a one-dimensional trap.) The minima are given by $x_0 = \pm\sqrt{d/2b}$, so that the motion can be described as approximately harmonic, with frequency $\omega_0 = \sqrt{4d/m}$, m being the ionic mass. The harmonic approximation can be adjusted by fixing d (and consequently ω_0) and conveniently choosing the parameter b, which is equivalent to varying the height of the barrier separating the two wells, $h = d^2/4b$.

(ii) We also assume that the parabolic approximation to the potential around each minimum is designed to contain (at least) the two lowest states of the harmonic oscillator described by the wavefunctions $\phi_i^{(n)}[x - (-1)^i x_0]$, with $n = 1, 2$ referring to the ground and first excited states of the harmonic oscillator and $i = 1, 2$ referring to the harmonic wells centred at $x = \mp x_0$.

(iii) Finally, we assume that the potential is such that state $\phi_1^{(n)}$ (of harmonic trap 1) is spatially close to state $\phi_2^{(n)}$ (of harmonic trap 2).

Thus, these local modes are not orthogonal, due to the overlap ϵ between the corresponding modes of the two wells:

$$\int \mathrm{d}x\, (\phi_i^{(n)}[x-(-1)^i x_0])^* \phi_j^{(m)}[x-(-1)^j x_0] = [\delta_{ij}+\epsilon(1-\delta_{ij})]\delta_{nm}. \quad (1)$$

When $\epsilon \ll 1$, given a first order correction, these local modes are approximately orthogonal and the eigenstates of the global double-well potential may be approximated by the symmetric and asymmetric superpositions $\phi_\pm^{(n)}(x) \approx [\phi_1^{(n)}(x+x_0) \pm \phi_2^{(n)}(x-x_0)]/\sqrt{2}$, with corresponding eigenvalues $E_\pm^{(n)} = E_0^{(n)} \pm \mathcal{R}^{(n)}$. The coupling constants between the local states are given by the matrix elements

$$\mathcal{R}^{(n)} = \int \mathrm{d}x\, [\phi_1^{(n)}(x+x_0)]^*[V(x)-\tilde{V}_1[x+x_0]]\phi_2^{(n)}(x-x_0), \quad (2)$$

where $\tilde{V}_i[x-(-1)^i x_0]$ indicate the parabolic potential approximations around $x = (-1)^i x_0$. The tunnelling frequencies $\Omega^{(n)}$ between the corresponding eigenstates in $\tilde{V}_1$ and $\tilde{V}_2$ are given by $\Omega^{(n)} = 2|\mathcal{R}^{(n)}|/\hbar$. In order to make the first order correction (ϵ^1) valid, ensuring that $\mathcal{R}^{(n)}/E_0^{(n)} \ll 1$, we further impose the condition $x_0^2/\Delta_x^2 \gg 1$. Scaling the length in units of the position uncertainty in a harmonic oscillator ground state $\Delta_x^2 = \hbar/(2m\omega_0)$, we obtain from equation (2) $\Omega^{(1)} = (3\omega_0 x_0^2/8\Delta_x^2)\exp(-x_0^2/2\Delta_x^2)$ and $\Omega^{(2)} = (x_0^2/\Delta_x^2)\Omega^{(1)}$.

The Hamiltonian describing the motional degrees of freedom of the ion trapped in the double-well potential described above is

$$\hat{H}_{motional} = \int \mathrm{d}x\, \hat{\Psi}^\dagger H \hat{\Psi}, \qquad H = -\frac{\hbar^2}{2m}\nabla^2 + V(x), \quad (3)$$

where $\hat{\Psi}(x) = \sum_{n,i} \phi_i^{(n)}(x)\hat{c}_i^{(n)}$ is the field operator which annihilates the ion in the state $\phi_i^{(n)}$, i.e., in energy level $E_0^{(n)}$ of the harmonic well $\tilde{V}_i$. From the eigenvalue equation $H\phi_\pm^{(n)} = E_\pm^{(n)}\phi_\pm^{(n)}$ and the assumption that $\epsilon \ll 1$, the Hamiltonian in equation (3) becomes

$$\hat{H}_{motional} = \sum_n [E_0^{(n)}(\hat{c}_1^{(n)\dagger}\hat{c}_1^{(n)} + \hat{c}_2^{(n)\dagger}\hat{c}_2^{(n)}) + \mathcal{R}^{(n)}(\hat{c}_1^{(n)\dagger}\hat{c}_2^{(n)} + \hat{c}_2^{(n)\dagger}\hat{c}_1^{(n)})]. \quad (4)$$

Next, we assume that the trapped ion has two effective electronic states, excited $|\uparrow\rangle$ and ground $|\downarrow\rangle$, separated by frequency ω and coupled by the interaction with an effective laser plane wave propagating in the x direction, with wavevector $k_L = \omega_L/c$. In this configuration, only the ionic motion along the x axis will be modified. The effective pumping laser beam is detuned by $\delta \equiv \omega - \omega_L$ from the $|\uparrow\rangle \leftrightarrow |\downarrow\rangle$ transition. In the NIST experiments with $^9Be^+$ the laser beams (with different frequencies) composing the effective pumping laser, are detuned from a third more excited level which, in the stimulated Raman-type configuration, is adiabatically eliminated [8]. In the Innsbruck experiments with $^{40}Ca^+$, a coherently driving direct transition between the electronic ground and excited states is employed [9]. A *probe* laser, strongly coupled to the transition between the electronic ground state and a third more excited level $|s\rangle$, is also employed in order to measure the ionic vibrational state by collecting the resonance fluorescence signal, which is the probability of the ion being found in the internal state $|\downarrow\rangle$.

We can follow the tunnelling phenomenon through the time evolution of the probability of fluorescence measurement of the electronic ground state collected in two different situations:

(a) by individual addressing the ion in harmonic well 1 or, what seems to be more attractive experimentally,
(b) by considering the laser beams (the pumping and the probe lasers) to reach both local potential wells simultaneously.

The ion–laser interaction Hamiltonian that describes the effective interaction of the quantized motion of the ionic centre of mass coupled to its electronic degrees of freedom is [8]

$$\hat{H}_{ion-laser} = \hbar g(\hat{\sigma}_+ \mathrm{e}^{\mathrm{i}k_L\hat{x}-\mathrm{i}\omega_L t+\mathrm{i}\varphi_L} + \hat{\sigma}_- \mathrm{e}^{-\mathrm{i}k_L\hat{x}+\mathrm{i}\omega_L t-\mathrm{i}\varphi_L}), \quad (5)$$

where $\sigma_+ = |\uparrow\rangle\langle\downarrow|$ and $\sigma_- = |\downarrow\rangle\langle\uparrow|$ are the usual Pauli pseudo-spin operators, g is the effective Rabi frequency of the transition $|\uparrow\rangle \leftrightarrow |\downarrow\rangle$ and ϕ_L is the phase difference between the two lasers composing the effective beam. Since, considering situation (a), the laser beams are disposed in harmonic well 1, the position operator $\hat{x}$ is given by

$$\hat{x} = \sum_{n,m}\int \mathrm{d}x\, \phi_1^{(n)^\dagger}(x)x\phi_1^{(m)}(x)\hat{c}_1^{(n)^\dagger}\hat{c}_1^{(m)} = \Delta_x \sum_n \sqrt{n+1}(\hat{c}_1^{(n)^\dagger}\hat{c}_1^{(n+1)} + \hat{c}_1^{(n+1)^\dagger}\hat{c}_1^{(n)}). \quad (6)$$

Evidently, considering situation (b) where the laser beams reach both local wells, the position operator turns out to be $\hat{x} = \Delta_x \sum_{j=1,2}\sum_n \sqrt{n+1}(\hat{c}_j^{(n)^\dagger}\hat{c}_j^{(n+1)} + \hat{c}_j^{(n+1)^\dagger}\hat{c}_j^{(n)})$.

In what follows we consider only situation (a) since the generalization for situation (b), which will be analysed further, is straightforward. In a frame rotating at the effective laser frequency ω_L, the ion–laser Hamiltonian is given by

$$\hat{H}_{ion-laser} = \hbar g\left[\hat{\sigma}_+ \exp\left(\mathrm{i}\eta\sum_n \sqrt{n+1}(\hat{c}_1^{(n)^\dagger}\hat{c}_1^{(n+1)} + \hat{c}_1^{(n+1)^\dagger}\hat{c}_1^{(n)}) + \mathrm{i}\varphi_L\right) + \mathrm{H.c.}\right], \quad (7)$$

where we have introduced the Lamb–Dicke parameter $\eta \equiv k_L\Delta_x$ and H.c. denotes the Hermitian conjugate.

We now rewrite the total Hamiltonian in the interaction picture (script font labels) via the unitary transformation $\hat{U}(t) = \exp(-\mathrm{i}\hat{H}_0 t)$, where $\hat{H}_0 = \sum_n E_0^{(n)}(\hat{c}_1^{(n)^\dagger}\hat{c}_1^{(n)} + \hat{c}_2^{(n)^\dagger}\hat{c}_2^{(n)}) + \hbar\frac{\delta}{2}\hat{\sigma}_z$ indicates the free Hamiltonian composed of the internal and motional degrees of freedom of the trapped ion, σ_z being the Pauli operator. The resulting Hamiltonian, including the motional and electronic degrees of freedom, reads

$$\hat{\mathcal{H}} = \sum_n \mathcal{R}^{(n)}(\hat{c}_1^{(n)^\dagger}\hat{c}_2^{(n)} + \hat{c}_2^{(n)^\dagger}\hat{c}_1^{(n)}) + \hbar g\exp\left(-\eta^2\sum_n \hat{c}_1^{(n)^\dagger}\hat{c}_1^{(n)}\right) \times \left\{\sigma_+ \exp\left[\mathrm{i}\eta\sum_n \sqrt{n+1}(\hat{c}_1^{(n)^\dagger}\hat{c}_1^{(n+1)}\mathrm{e}^{-\mathrm{i}\omega_0 t} + \hat{c}_1^{(n+1)^\dagger}\hat{c}_1^{(n)}\mathrm{e}^{\mathrm{i}\omega_0 t})\right]\mathrm{e}^{\mathrm{i}\delta t+\mathrm{i}\varphi_L} + \mathrm{H.c.}\right\}. \quad (8)$$

In order to simplify the expression (8)

(i) we adjust the ion–laser detuning to the first red sideband for the ion–laser interaction ($\delta = \omega_0$),

(ii) the assumption of the standard Lamb–Dicke limit ($\eta \ll 1$), where the ionic centre of mass is strongly localized with respect to the laser wavelength, enables the expansion of the Hamiltonian (8) to first order correction (η^1),

(iii) with the optical rotating wave approximation, we obtain the expression

$$\hat{\mathcal{H}} = \sum_n \mathcal{R}^{(n)}(\hat{c}_1^{(n)^\dagger}\hat{c}_2^{(n)} + \hat{c}_2^{(n)^\dagger}\hat{c}_1^{(n)}) + \mathrm{i}\hbar\eta g \exp\left(-\eta^2 \sum_n \hat{c}_1^{(n)^\dagger}\hat{c}_1^{(n)}\right) \times \left(\sigma_+ \sum_n \sqrt{n+1}\hat{c}_1^{(n)^\dagger}\hat{c}_1^{(n+1)}\mathrm{e}^{+\mathrm{i}\varphi_L} - \mathrm{H.c.}\right), \tag{9}$$

which in the absence of the tunnelling mechanism leads to the coupling between the electronic and motional degrees of freedom of the trapped ion, described by the Jaynes–Cummings Hamiltonian (JCH).

At this point, we assume that the ion is initially cooled to its motional ground state in harmonic well 1, and laser-excited to the electronic state $|\uparrow\rangle$. Thus, the JCH induces the transition $|1,0\rangle_1|\uparrow\rangle \leftrightarrow |0,1\rangle_1|\downarrow\rangle$, where the ket $|1,0\rangle_l$ ($|0,1\rangle_l$) indicates the ion in the motional ground (excited) state of $\tilde{V}_l$. Evidently, being in the motional state $|1,0\rangle_1$ ($|0,1\rangle_1$), the ion has a finite probability of tunnelling to the corresponding state of $\tilde{V}_2$: $|1,0\rangle_2$ ($|0,1\rangle_2$). Therefore, the motional basis states of the process are restricted to the ground and first excited states of the harmonic traps, which is why we assumed from the beginning that the parabolic approximation to the potential around each minimum is designed to contain (at least) the two lowest states of the harmonic oscillator. By collecting the resonance fluorescence signal in $\tilde{V}_1$, we can probe the tunnelling mechanism through the behaviour of the function $\mathsf{P}_\downarrow(t)$, the probability of fluorescence measurement of the electronic ground state.

Considering the Lamb–Dicke limit and the fact that we have only one particle in the process, the function $\exp(-\eta^2 \sum_n \hat{c}_1^{(n)^\dagger}\hat{c}_1^{(n)})$ can be fairly approximated by unity, so the Hamiltonian governing the process has the simplified form (for $n = 1, 2$)

$$\hat{\mathcal{H}} = \mathcal{R}^{(1)}(\hat{c}_1^{(1)^\dagger}\hat{c}_2^{(1)} + \hat{c}_1^{(1)}\hat{c}_2^{(1)^\dagger}) + \mathcal{R}^{(2)}(\hat{c}_1^{(2)^\dagger}\hat{c}_2^{(2)} + \hat{c}_1^{(2)}\hat{c}_2^{(2)^\dagger}) + \mathrm{i}\hbar\eta g(\sigma_+\hat{c}_1^{(1)^\dagger}\hat{c}_1^{(2)}\mathrm{e}^{+\mathrm{i}\varphi_L} - \sigma_-\hat{c}_1^{(1)}\hat{c}_1^{(2)^\dagger}\mathrm{e}^{-\mathrm{i}\varphi_L}). \tag{10}$$

Before proceeding further, it is worth mentioning that instead of adjusting the ion–laser detuning to the first red sideband for the ion–laser interaction ($\delta = \omega_0$), we could have chosen the carrier interaction where $\delta = 0$. In this case the effective Hamiltonian following from equation (8) (with the above-mentioned approximations) simplifies to

$$\hat{\mathcal{H}}_{carrier} = \mathcal{R}^{(1)}(\hat{c}_1^{(1)^\dagger}\hat{c}_2^{(1)} + \hat{c}_1^{(1)}\hat{c}_2^{(1)^\dagger}) + \mathcal{R}^{(2)}(\hat{c}_1^{(2)^\dagger}\hat{c}_2^{(2)} + \hat{c}_1^{(2)}\hat{c}_2^{(2)^\dagger}) + \hbar g(\sigma_+\mathrm{e}^{+\mathrm{i}\varphi_L} + \sigma_-\mathrm{e}^{-\mathrm{i}\varphi_L}). \tag{11}$$

We note that the Pauli operators act only when the ion is in harmonic well 1. The dynamics governed by Hamiltonians (10) and (11) make it possible to probe the tunnelling mechanism of the ion by collecting resonance fluorescence signals, as discussed above.

Starting from the initial state $|1,0\rangle_1|0,0\rangle_2|\uparrow\rangle$ and Hamiltonian (10) we obtain from the Schrödinger evolution the evolved state

$$|\psi(t)\rangle = [\mathcal{C}_1^{(1)}(t)|1,0\rangle_1|0,0\rangle_2 + \mathcal{C}_2^{(1)}(t)|0,0\rangle_1|1,0\rangle_2]|\uparrow\rangle + [\mathcal{C}_1^{(2)}(t)|0,1\rangle_1|0,0\rangle_2 + \mathcal{C}_2^{(2)}(t)|0,0\rangle_1|0,1\rangle_2]|\downarrow\rangle, \tag{12}$$

whose coefficients satisfy the set of coupled linear equations

$$\mathrm{i}\hbar\frac{\mathrm{d}}{\mathrm{d}t}\mathcal{C}_1^{(n)}(t) = \mathcal{R}^{(n)}\mathcal{C}_2^{(n)}(t) - (-1)^n\mathrm{i}\hbar\eta g\mathrm{e}^{-(-1)^n\mathrm{i}\varphi_L}\mathcal{C}_1^{(m)}(t), \tag{13a}$$

$$\mathrm{i}\hbar\frac{\mathrm{d}}{\mathrm{d}t}\mathcal{C}_2^{(n)}(t) = \mathcal{R}^{(n)}\mathcal{C}_1^{(n)}(t), \tag{13b}$$

with $n, m = 1, 2$ ($n \neq m$) and initial conditions $\mathcal{C}_1^{(1)}(0) = 1$, $\mathcal{C}_2^{(1)}(0) = \mathcal{C}_1^{(2)}(0) = \mathcal{C}_2^{(2)}(0) = 0$. Now, we introduce a further simplification into the present scheme. The larger the ratio x_0^2/Δ_x^2 obtained by engineering the trap, the smaller becomes the ratio of the matrix elements $|\mathcal{R}^{(1)}/\mathcal{R}^{(2)}|$. Therefore, when $|\mathcal{R}^{(1)}/\mathcal{R}^{(2)}| \ll 1$, we can neglect the tunnelling process between the ground states in the two harmonic wells. In this case, the first term in Hamiltonian (10) can be disregarded and, by adjusting the phase of the laser pulse such that $\varphi_L = -\pi/2$, we obtain the coefficients:

$$\mathcal{C}_1^{(1)}(t) = [\cos(\xi\mathsf{w}t) + \xi^2 - 1]/\xi^2, \qquad \mathcal{C}_2^{(1)}(0) = 0, \tag{14a}$$

$$\mathcal{C}_1^{(2)}(t) = \mathrm{i}\sin(\xi\mathsf{w}t)/\xi, \qquad \mathcal{C}_2^{(2)}(0) = \sqrt{\xi^2 - 1}[\cos(\xi\mathsf{w}t) - 1]/\xi^2, \tag{14b}$$

where the effective Rabi frequency, $\mathsf{w} = \eta g$, is modified by the parameter $\xi = \{1 + [\mathcal{R}^{(2)}/(\hbar\eta g)]^2\}^{1/2}$. Next we analyzer the influence of parameter ξ on the time evolution of the probability of measuring fluorescence of the electronic ground state $\mathsf{P}_\downarrow(t) = |\mathcal{C}_1^{(2)}(t)|^2$ in harmonic well 1. Evidently, when $\mathcal{R}^{(2)} = 0$, we recover the well-known dynamics of $P_\downarrow(t)$ for JCH [8]. For the choice $\mathcal{R}^{(2)}/(\hbar\eta g) = 1$ ($\xi = \sqrt{2}$) and employing the typical values in experiments with $^{40}Ca^+$ [9, 10], $\eta \approx 0.1$, $g \approx 200$ kHz and $\omega_0 \approx 2$ MHz (giving the estimate $\mathcal{R}^{(2)}/(\hbar\eta g) \approx 150 \times \mathcal{R}^{(2)}/E_0^{(2)}$), we obtain $\mathcal{R}^{(2)}/E_0^{(2)} \approx 7 \times 10^{-3}$ as required to justify the approximation that the superpositions $\phi_\pm^n(x)$ constitute eigenstates of the global double-well potential. In fact, remembering that $\mathcal{R}^{(2)}/(\hbar\eta g) = (3\omega_0 x_0^4/16\eta g\Delta_x^4)\exp(-x_0^2/2\Delta_x^2)$, we obtain from the previous parameters the values $x_0^2/\Delta_x^2 \approx 17.3$ and $|\mathcal{R}^{(1)}/\mathcal{R}^{(2)}| \approx 6 \times 10^{-2}$, which are in agreement with the approximations considered above. In figure 1 we display the behaviour of function $\mathsf{P}_\downarrow(t)$ for $\mathcal{R}^{(2)}/(\hbar\eta g) = 0$ ($\xi = 1$, corresponding to the dynamics of the JCH) and $\mathcal{R}^{(2)}/(\hbar\eta g) = 1$. As anticipated by observing the expression for $\mathsf{P}_\downarrow(t)$, the increase in the tunnelling rate $\mathcal{R}^{(2)}$ leads to an increase in the effective frequency $\xi\mathsf{w}$ of population inversion and, conversely, a decrease in the amplitude of the oscillations of $\mathsf{P}_\downarrow(t)$, clearly indicating the tunnelling process. In fact, as soon as the ion reaches the excited state of local well 1, the coupling $\mathcal{R}^{(2)}$ to local well 2 entangles the motional excited states of both wells, preventing the probability $\mathsf{P}_\downarrow(t)$ (associated with the measurement of state $|0,1\rangle_1|\downarrow\rangle$) from reaching unity. When the curve in figure 1 for $\mathcal{R}^{(2)}/(\hbar\eta g) = 1$ reaches its maxima ($\mathsf{w}t = n\pi\sqrt{2}/4, n = 1, 2, \ldots$), we have the entangled state $\frac{1}{2}|1,0\rangle_1|0,0\rangle_2|\uparrow\rangle + (\frac{\mathrm{i}}{\sqrt{2}}|0,1\rangle_1|0,0\rangle_2 - \frac{1}{2}|0,0\rangle_1|0,1\rangle_2)|\downarrow\rangle$.

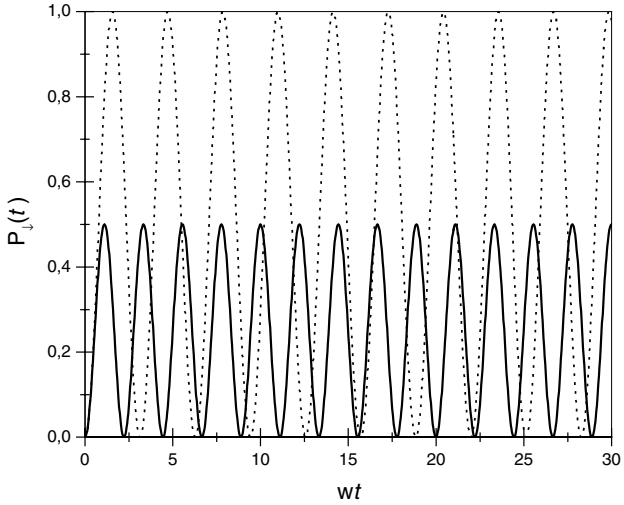

Figure 1. The evolution of function $\mathsf{P}_{\downarrow}(t)$, in the Jaynes–Cummings regime and individual addressing of local well 1, for the values $\mathcal{R}^{(2)}/(\hbar\eta g) = 0$ (dotted curve) and 1 (full curve).

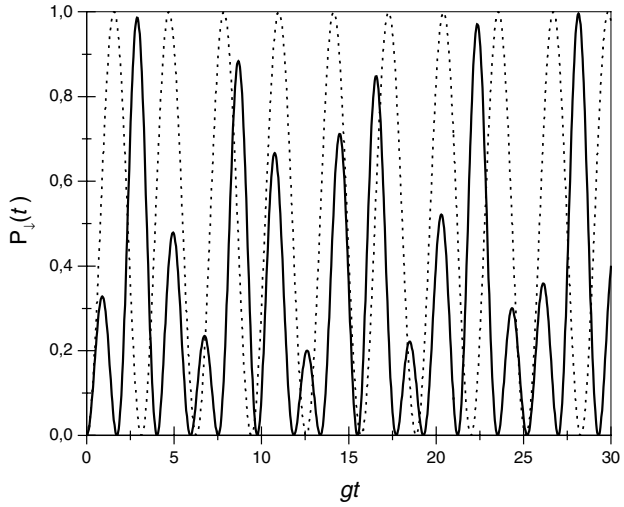

Figure 2. The evolution of function $\mathsf{P}_{\downarrow}(t)$, in the carrier regime and individual addressing of local well 1, for the values $\mathcal{R}^{(2)}/(\hbar g) = 0$ (dotted curve) and 1 (full curve).

Therefore, both characteristics, the effective frequency $\xi\mathsf{w}$ of population inversion and the amplitude of the oscillations of $\mathsf{P}_{\downarrow}(t)$, can be used to probe the single-particle tunnelling mechanism.

It is worth observing that the choice of the alternative initial state $|0,1\rangle_1|0,0\rangle_2|\downarrow\rangle$ leads to the entanglement $(|1,0\rangle_1|0,0\rangle_2|\uparrow\rangle + |0,0\rangle_1|0,1\rangle_2|\downarrow\rangle)/\sqrt{2}$. In this situation, as expected for a closed system, we can re-establish a value of unity for $\mathsf{P}_{\downarrow}(t)$.

Now, turning to the Hamiltonian (11) and solving the Schrödinger equation for the initial state $|0,1\rangle_1|0,0\rangle_2|\uparrow\rangle$, we obtain the result

$$\mathsf{P}_{\downarrow}(t) = \frac{(\lambda_1 \sin(\lambda_1 gt) - \lambda_2 \sin(\lambda_2 gt))^2}{(\lambda_2^2 - \lambda_1^2)^2}, \qquad (15)$$

where the parameters modifying the Rabi frequency, g, are $\lambda_i = \frac{1}{\sqrt{2}}\{1 + 2[\mathcal{R}^{(2)}/(\hbar g)]^2 + (-1)^i[1 + 4[\mathcal{R}^{(2)}/(\hbar g)]^2]^{1/2}\}^{1/2}$. Evidently, when $\mathcal{R}^{(2)} = 0$, we get the usual dynamics for the carrier pulse, with $\mathsf{P}_{\downarrow}(t) = |\sin(gt)|^2$. In figure 2 we display the time evolution of equation (15), for $\mathcal{R}^{(2)}/(\hbar g) = 0$ and $\mathcal{R}^{(2)}/(\hbar g) = 1$ ($\lambda_i = [(3 + (-1)^i\sqrt{5})/2]^{1/2}$). For the typical values given above, we obtain $\mathcal{R}^{(2)}/E_0^{(2)} \approx 7 \times 10^{-2}$ (a value which matches $x_0^2/\Delta_x^2 \approx 10.8$ and $|\mathcal{R}^{(1)}/\mathcal{R}^{(2)}| \approx 0.1$). As with the behaviour displayed in figure 1, we observe that the frequency of population inversion is higher than the Rabi frequency g associated with free carrier dynamics. However, in contrast to the situation in figure 1, the probability $\mathsf{P}_{\downarrow}(t)$ (displaying the characteristic beat pattern due to equation (15)) can still reach unity. Since in the carrier regime the electronic states do not couple to the motional states, the excited and ground electronic states are both subject to the tunnelling process (different from the JCH case), resulting in the interference pattern shown in figure 2.

From the value for the position uncertainty in a harmonic oscillator ground state $\Delta_x^2 = \hbar/(2m\omega_0)$ computed for $^{40}Ca^+$ with motional frequency $\omega_0 \approx 2$ MHz, and considering the Jaynes–Cummings regime, where $x_0^2/\Delta_x^2 \approx 17.3$, we obtain (using the typical values $\eta \approx 0.1$ and $g \approx 200$ kHz [9, 10]) the distance between the local minima $2x_0 \approx 0.16$ μm. Making the same estimates for the carrier regime, where $x_0^2/\Delta_x^2 \approx 10.3$, we obtain the distance between the local minima $2x_0 \approx 0.13$ μm. Recently, laser addressing of individual ions was reported [10] in a linear ion trap with frequency 125 kHz when the distance between the ions is about 19 μm. The authors of [10] argue that the addressing technique presented permits individual addressing when the distance between the ions is only 7.6 μm with small error. Therefore, with current technology it is difficult to individually address each local potential well. On the other hand, when considering the situation (b) where the laser beams reach the local wells simultaneously, the Hamiltonian (10) (in the Jaynes–Cummings regime and assuming $|\mathcal{R}^{(1)}/\mathcal{R}^{(2)}| \ll 1$) turns to be

$$\begin{aligned}\hat{\mathcal{H}} = {} & \mathcal{R}^{(2)}(\hat{c}_1^{(2)^\dagger}\hat{c}_2^{(2)} + \hat{c}_1^{(2)}\hat{c}_2^{(2)^\dagger}) \\ & + \mathrm{i}\hbar\eta g[\sigma_+(\hat{c}_1^{(1)^\dagger}\hat{c}_1^{(2)} + \hat{c}_2^{(1)^\dagger}\hat{c}_2^{(2)})\mathrm{e}^{+\mathrm{i}\varphi_L} \\ & - \sigma_-(\hat{c}_1^{(1)}\hat{c}_1^{(2)^\dagger} + \hat{c}_2^{(1)}\hat{c}_2^{(2)^\dagger})\mathrm{e}^{-\mathrm{i}\varphi_L}]. \qquad (16)\end{aligned}$$

Starting from the initial state $|1,0\rangle_1|0,0\rangle_2|\uparrow\rangle$ and Hamiltonian (16) we obtain from the Schrödinger evolution the evolved state described by equation (12) with the coefficients satisfying the coupled linear equations

$$\mathrm{i}\hbar\frac{\mathrm{d}}{\mathrm{d}t}\mathcal{C}_n^{(1)} = \mathrm{i}\hbar g\mathrm{e}^{\mathrm{i}\varphi_L}\mathcal{C}_n^{(2)}(t), \qquad (17a)$$

$$\mathrm{i}\hbar\frac{\mathrm{d}}{\mathrm{d}t}\mathcal{C}_n^{(2)}(t) = \mathcal{R}^{(2)}\mathcal{C}_m^{(2)}(t) - \mathrm{i}\hbar g\mathrm{e}^{-\mathrm{i}\varphi_L}\mathcal{C}_n^{(1)}(t), \qquad (17b)$$

with $n, m = 1, 2$ ($n \neq m$) and initial conditions $\mathcal{C}_1^{(1)}(0) = 1$, $\mathcal{C}_2^{(1)}(0) = \mathcal{C}_1^{(2)}(0) = \mathcal{C}_2^{(2)}(0) = 0$. Solving the system above we obtain the coefficients:

$$\mathcal{C}_1^{(1)}(t) = \frac{1}{(\chi^2 + 4)}\sum_{j=1,2}[\chi^2 - (\lambda_j)^2 + 3]\cos(\lambda_j gt), \qquad (18a)$$

$$\begin{aligned}\mathcal{C}_2^{(1)}(t) = {} & \frac{\mathrm{i}}{\chi(\chi^2 + 4)} \\ & \times \sum_{j=1,2}\lambda_j[(\chi^2 + 2)^2 - (\chi^2 + 2)(\lambda_j)^2]\sin(\lambda_j gt), \qquad (18b)\end{aligned}$$

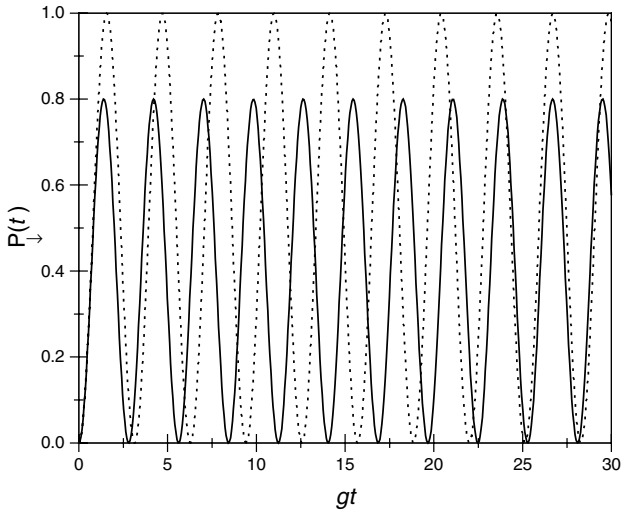

Figure 3. The evolution of function $\mathsf{P}_{\downarrow}(t)$, in the Jaynes–Cummings regime and the laser beams reaching both local wells simultaneously, for the values $\mathcal{R}^{(2)}/(\hbar\eta g) = 0$ (dotted curve) and 1 (full curve).

$$\mathcal{C}_1^{(2)}(t) = \frac{\mathrm{e}^{-\mathrm{i}\varphi_L}}{(\chi^2+4)} \sum_{j=1,2} \lambda_j [(\lambda_j)^2 - \chi^2 - 3] \sin(\lambda_j g t), \quad (18c)$$

$$\mathcal{C}_2^{(2)}(t) = \frac{-\mathrm{i}\mathrm{e}^{-\mathrm{i}\varphi_L}}{\chi(\chi^2+4)} \sum_{j=1,2} [2(\lambda_j)^2 - \chi^2 - 2] \cos(\lambda_j g t), \quad (18d)$$

where $\lambda_j = \{1 + [\chi^2 + (-1)^j \chi\sqrt{4+\chi^2}]/2\}^{1/2}$ and $\chi = \mathcal{R}^{(2)}/\hbar\eta g$. The probability of measuring the electronic ground state $|\downarrow\rangle$ of the ion in both local wells 1 and 2 is given by $\mathsf{P}_{\downarrow}(t) = |\mathcal{C}_1^{(2)}(t) + \mathcal{C}_2^{(2)}(t)|^2$. In figure 3 we display the behaviour of function $\mathsf{P}_{\downarrow}(t)$ for $\mathcal{R}^{(2)}/(\hbar\eta g) = 0$ (corresponding to the well-known Jaynes–Cummings dynamics) and $\mathcal{R}^{(2)}/(\hbar\eta g) = 1\big(\lambda_1 = \sqrt{3-\sqrt{5}/2}$ and $\lambda_2 = \sqrt{3+\sqrt{5}/2}\big)$. As with the behaviour displayed in figure 1, we observe that the frequency of population inversion in figure 3 (full curve) is higher than the Rabi frequency g associated with the free JCH dynamics whereas the amplitude of the oscillations of $\mathsf{P}_{\downarrow}(t)$ is smaller than that for the free JCH dynamics. Both characteristics clearly indicate the tunnelling process in figure 3, without the requirement of the individual addressing of each local potential well.

In conclusion, we have presented a scheme for probing the tunnelling process of a single ion trapped in a double-well electromagnetic potential. The tunnelling dynamics are characterized by the behaviour of the probability of collecting an electronic ground state fluorescence signal in one of the local potential wells. Two situations were analysed when collecting fluorescence measurements

(a) individual addressing the ion in harmonic well 1, and
(b) considering the laser beams to reach the local wells simultaneously.

Although the situation (a) is beyond current technology, single-particle quantum tunnelling can clearly be probed through the situation (b). Considering the possibility of individual addressing of local wells, the present proposal can be extended to the implementation of a fundamental controlled-NOT two-bit gate by adding another laser beam in harmonic well 2 and storing the quantum bits in the motional states of both local wells [11]. We also note that our proposal can be implemented in spite of the decoherence processes coming from the coupling of the motional modes with the residual background gas [12] and with classical stochastic electric field [13], in addition to the finite lifetime of the electronic levels [13, 14]. From the experimental results reported in [8, 9] we observe that several Rabi oscillations are visible within the decoherence time making it possible to observe the signature of the tunnelling process. However, we stress that the designing of the double-well potential would require that the trap electrodes be only a few micron away from the ion. It is then likely that the heating rate in the trap would become higher than that observed in single traps, increasing the decoherence rate [15]. Besides, the required trap structure makes it difficult to obtain high trap frequencies (about 1 MHz) and consequently, makes the cooling process of the ion to its motional ground state difficult [15]. Here we note that the cooling process could be implemented in a single trap structure which could be adiabatically modified to a double-well potential.

Although the design of such a double-well trap may turn out to be a considerable technical challenge, the fundamental principles discussed here can be implemented by engineering two-mode interactions in ion traps [16], in which the motional states of the ion in two different directions can be coupled, analogously to the dynamics for the double-well. In addition, the proposal presented here might provide a motivation for future experimental work.

Acknowledgments

We wish to express thanks for the support from FAPESP (under contracts nos 99/11617-0, 00/15084-5, and 02/02633-6) and CNPq (Intituto do Milênio de Informação Quântica), Brazilian agencies. We also thank Christian Roos for helpful discussions.

References

[1] Cirac J I, Zoller P, Kimble H J and Mabuchi H 1997 *Phys. Rev. Lett.* **78** 3221
Pellizzari T 1997 *Phys. Rev. Lett.* **79** 5242
[2] Cirac J I and Zoller P 1995 *Phys. Rev. Lett.* **74** 4091
Turchette Q A, Hood C J, Lange W, Mabuchi H and Kimble H J 1995 *Phys. Rev. Lett.* **75** 4710
Chuang I L, Vandersypen L M K, Zhou X L, Leung D W and Lloyd S 1998 *Nature* **393** 143
Kane B E 1998 *Nature* **393** 143
Vandersypen L M K, Steffen M, Breyta G, Yannoni C S, Sherwood M H and Chuang I L 2001 *Nature* **414** 883
[3] Einstein A, Podolsky B and Rosen N 1935 *Phys. Rev.* **47** 777
[4] Caldeira A O and Leggett A J 1981 *Phys. Rev. Lett.* **46** 211
[5] Leggett A J, Chakravarty S, Dorsey A T, Fisher M P A, Garg A and Zwerger W 1987 *Rev. Mod. Phys.* **59** 1
[6] Milburn G J, Corney J, Wright E M and Walls D F 1997 *Phys. Rev.* A **55** 4318
Corney J F and Milburn G J 1998 *Phys. Rev.* **58** 2399
[7] Andrews M R, Townsend C G, Miesner H J, Durfee D S, Kurn D M and Ketterle W 1997 *Science* **275** 637
[8] Wineland D J, Monroe C, Itano W M, Leibfried D, King B E and Meekhof D M 1998 *J. Res. NIST* **103** 259
[9] Roos Ch, Zeiger Th, Rohde H, Nägerl H. C, Eschner J, Leibfried D, Schmidt-Kaler F and Blatt R 1999 *Phys. Rev. Lett.* **83** 4713

[10] Nägerl H C, Leibfried D, Rohde H, Thalhammer G, Eschner J, Schmidt-Kaler F and Blatt R 1999 *Phys. Rev.* A **60** 145
[11] Serra R M *et al*, to be published elsewhere
[12] Serra R M, de Almeida N G, da Costa W B and Moussa M H Y 2001 *Phys. Rev.* A **64** 033419
[13] Budini A A, de Matos Filho R L and Zagury N 2002 *Phys. Rev.* A **65** 041402
[14] Di Fidio C and Vogel W 2000 *Phys. Rev.* A **62** 031802(R)
[15] Roos Ch 2003 private communication
[16] Steinbach J, Twamley J and Knight P L 1997 *Phys. Rev.* A **56** 4815